

# Photon Structure Function <sup>\*</sup>

Rohini M. Godbole<sup>†‡</sup>

*Center for Theoretical Studies, Indian Institute of Science, Bangalore, 560 012, India.*

## Abstract

After briefly explaining the idea of photon structure functions ( $F_2^\gamma$ ,  $F_L^\gamma$ ) I review the current theoretical and experimental developments in the subject of extraction of  $\bar{q}^\gamma$  from a study of the Deep Inelastic Scattering (DIS). I then end by pointing out recent progress in getting information about the parton content of the photon from hard processes other than DIS.

## Introduction:

The photon is the simplest of all bosons. Quantum Electrodynamics (QED), the theory of  $e - \gamma$  interactions is the most accurately tested field theory we have. At first sight therefore it is surprising that many reactions involving (quasi-)real photons are much less well understood, both theoretically and experimentally. This outwardly strange fact is the result of fluctuations of a photon into quark-antiquark pairs. Whenever the lifetime of the virtual state exceeds the typical hadronic time scale the (virtual)  $q\bar{q}$  pair has sufficient time to evolve into a complicated hadronic state that cannot be described by perturbative methods only. Even if the lifetime is shorter, hard gluon emission and related processes complicate the picture substantially. This thus endows the photon with a hadronic structure so to say.

The understanding of these virtual hadronic states becomes particularly important when they are “kicked on the mass shell” by an interaction of the photon. The most thoroughly studied reactions of this type involve interactions of a real and a virtual photon (e.g. in  $e\gamma$  scattering); of two real photons ( $\gamma\gamma$  scattering at  $e^+e^-$  colliders), the so called Deep Inelastic Scattering (DIS) off a photon target. There are two very important reasons for us to be interested in the study of hadronic structure of the photon; one is to facilitate better understanding of the interactions of high energy photons which can help sharpen our assesment of backgrounds at high energy colliders; this is true for high-energy linear  $e^+e^-$  colliders that are now being discussed, and especially for the so-called  $\gamma\gamma$  colliders

---

<sup>\*</sup>Invited talk at the XI DAE Symposium, Santiniketan, Jan. 95

<sup>†</sup>On leave from Dept. of Physics, University of Bombay, Bombay, India.

<sup>‡</sup>E-mail : rohini@cts.iisc.ernet.in

and second is the unique opportunity that the photon provides to study the perturbative and nonperturbative aspects of QCD. The latter is due to the fact that “in principle” the hadronic structure of the photon arises from the “hard”  $\gamma q\bar{q}$  vertex.

I discuss below mainly the DIS. These were the first photonic reactions for which predictions were made in the framework of the quark parton model (QPM) [1] and within QCD [2].  $e\gamma$  scattering was also among the first of the “hard” photonic reactions, which can at least partly be described by perturbation theory, to be studied experimentally [3]. After that in the end I will discuss in brief how one can use the ‘resolved photon’ processes [4] to probe the structure of the photon and mention some new experimental data which fortells the expected progress in the area.

### Photon Structure Functions:

Deep-inelastic  $e\gamma$  scattering (DIS), is theoretically very clean, being fully inclusive; it is thus well suited to serve as the defining process for photon structure functions and the parton content of the photon. See Ref.[5] for a pedagogical introduction to the subject.

Formally deep-inelastic  $e\gamma$  scattering is quite similar to  $ep$  scattering

$$e\gamma \rightarrow eX, \tag{1}$$

where  $X$  is any hadronic system and the squared four momentum transfer  $Q^2 \equiv -q^2 \geq 1 \text{ GeV}^2$ . The basic kinematics is explained in Fig. 1. The differential cross section can be

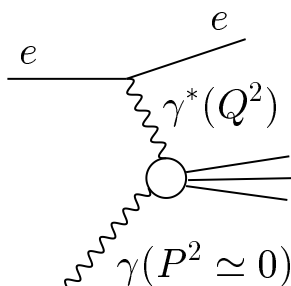


Figure 1: Deep Inelastic Scattering off a photon target.

written in terms of the scaling variables  $x \equiv Q^2/(2p \cdot q)$  and  $y \equiv Q^2/(sx)$ , where  $\sqrt{s}$  is the total available centre-of-mass (cms) energy:

$$\frac{d^2\sigma(e\gamma \rightarrow eX)}{dx dy} = \frac{2\pi\alpha_{\text{em}}^2 s}{Q^4} \left\{ [1 + (1 - y)^2] F_2^\gamma(x, Q^2) - y^2 F_L^\gamma(x, Q^2) \right\}; \tag{2}$$

this expression is completely analogous to the equation defining the protonic structure functions  $F_2$  and  $F_L$  in terms of the differential cross-section for  $ep$  scattering via the exchange of a virtual photon. The special significance [1] of  $e\gamma$  scattering lies in the fact that, while (at present) the  $x$ -dependence of the nucleonic structure functions can only be parametrized

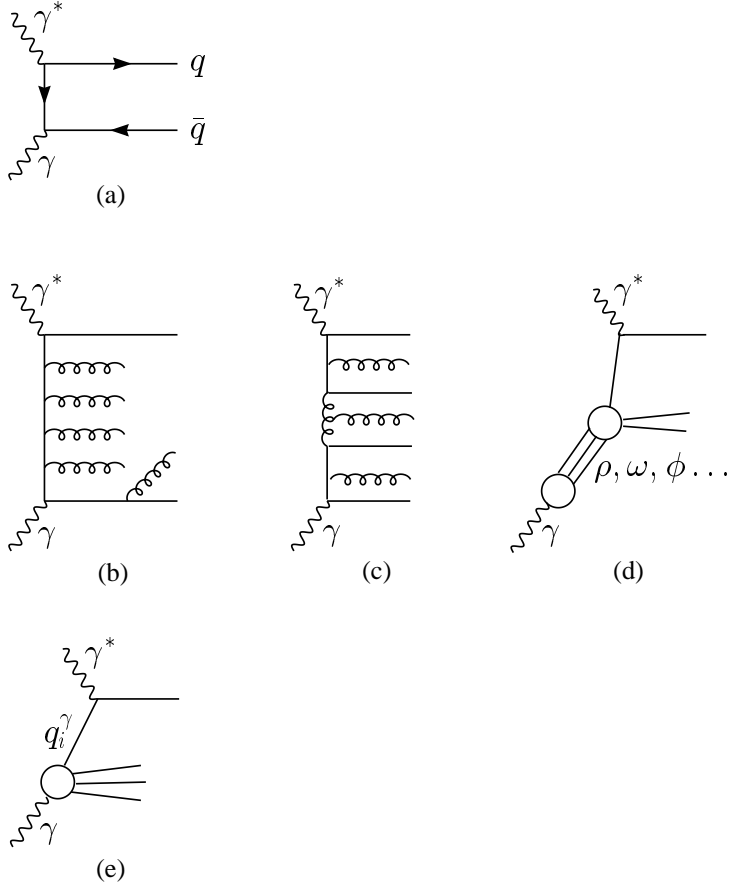


Figure 2: Different contributions to  $F_2^\gamma$

from data, the structure functions appearing in eq.(2) can be *computed* in the QPM from the diagram shown in Fig. 2a:

$$F_2^{\gamma, \text{QPM}}(x, Q^2) = \frac{3\alpha_{\text{em}}}{\pi} x \sum_q e_q^4 \left\{ [x^2 + (1-x)^2] \log \frac{W^2}{m_q^2} + 8x(1-x) - 1 \right\}, \quad (3a)$$

$$F_L^{\gamma, \text{QPM}}(x, Q^2) = \frac{3\alpha_{\text{em}}}{4\pi} \sum_q e_q^4 4x^2(1-x). \quad (3b)$$

where we have introduced the squared cms energy of the  $\gamma^*\gamma$  system

$$W^2 = Q^2 \left( \frac{1}{x} - 1 \right). \quad (4)$$

The sum in eq.(3) runs over all quark flavours, and  $e_q$  is the electric charge of quark  $q$  in units of the proton charge. Note that unlike the case of the proton, for the photon  $F_L^\gamma$  is nonzero even in the QPM.

Unfortunately, eq.(3) depends on the quark masses  $m_q$ . If this ansatz is to describe data [6] even approximately, one has to use constituent quark masses of a few hundred MeV here;

constituent quarks are not very well defined in field theory. Moreover, we now know that QPM predictions can be modified substantially by QCD effects. In case of  $e\gamma$  scattering, QCD corrections are described by the kind of diagrams shown in Figs. 2b,c. Diagrams of the type 2b leave the flavour structure unchanged and are therefore part of the (flavour) nonsinglet contribution to  $F_2^\gamma$ , while diagrams with several disconnected quark lines, as in Fig. 2c, contribute to the (flavour) singlet part of  $F_2^\gamma$ .

The interest in photon structure functions received a boost in 1977, when Witten showed [2] that such diagrams can be computed exactly, at least in the so-called ‘‘asymptotic’’ limit of infinite  $Q^2$ . Including next-to-leading order (NLO) corrections [7], the result can be written as

$$F_2^{\gamma,\text{asympt}}(x, Q^2) = \alpha_{\text{em}} \left[ \frac{1}{\alpha_s(Q^2)} a(x) + b(x) \right], \quad (5)$$

where  $a$  and  $b$  are *calculable* functions of  $x$ . The absolute normalization of this ‘‘asymptotic’’ solution is therefore given uniquely by  $\alpha_s(Q^2)$ , i.e. by the value of the QCD scale parameter  $\Lambda_{\text{QCD}}$ . It was therefore hoped that eq.(5) might be exploited for a very precise measurement of  $\Lambda_{\text{QCD}}$ .

Unfortunately this no longer appears feasible. One problem is that, in order to derive eq.(5), one has to neglect terms of the form  $\left(\frac{\alpha_s(Q^2)}{\alpha_s(Q_0^2)}\right)^P$ , where  $Q_0^2$  is some input scale (see below). Neglecting such terms is formally justified if  $\alpha_s(Q^2) \ll \alpha_s(Q_0^2)$  and  $P$  is positive. Unfortunately the first inequality is usually not satisfied at experimentally accessible values of  $Q^2$ , assuming  $Q_0^2$  is chosen in the region of applicability of perturbative QCD, i.e.  $\alpha_s(Q_0^2)/\pi \ll 1$ . Worse yet,  $P$  can be zero or even negative! In this case ignoring such terms is obviously a bad approximation. Indeed, one finds that eq.(5) contains divergencies as  $x \rightarrow 0$  [2, 7]:

$$a(x) \sim x^{-0.59}, \quad b(x) \sim x^{-1}. \quad (6)$$

The coefficient of the  $1/x$  pole in  $b$  is *negative*; eq.(5) therefore predicts negative counting rates at small  $x$ . Notice that the divergence is worse in the NLO contribution  $b$  than in the LO term  $a$ . It can be shown [8] that this trend continues in yet higher orders. Clearly the ‘‘asymptotic’’ solution is not a very useful concept, having a violently divergent perturbative expansion.

The worst divergencies in  $F_2^{\gamma,\text{asympt}}$  occur in the singlet sector, i.e. originate from diagrams of the type shown in Fig. 2c. There exist also non-perturbative contributions to  $F_2^\gamma$  which are traditionally estimated using the vector dominance model (VDM) [9], from the diagrams shown in Fig. 2d and we have

$$F_2^{\gamma,\text{VDM}} \propto F_2^{\rho,\omega,\phi} \simeq F_2^{\pi(p)}$$

Hence one expects the contribution of Fig. 2d to be well-behaved, i.e. non-singular. Hence this *cannot* cancel the divergencies of the ‘‘asymptotic’’ solution.

This discussion tells us that we cannot hope to compute  $F_2^\gamma(x, Q^2)$  from perturbation theory alone. The only meaningful approach seems to be that suggested by Glu'ck and Reya [10]. That is, one *formally* sums the contributions from Figs. 2a–d into the single diagram of Fig. 2e, where we have introduced quark densities in the photon  $q_i^\gamma(x, Q^2)$  such that (in LO)

$$F_2^\gamma(x, Q^2) = 2x \sum_i e_q^2 q_i^\gamma(x, Q^2), \quad (7)$$

where the sum runs over flavours,  $e_{q_i}$  is the electric charge of quark  $q_i$  in units of the proton charge, and the factor of 2 takes care of anti-quarks. This is merely a definition. In the approach of ref.[10] one does not attempt to compute the absolute size of the quark densities inside the photon. Rather, one introduces input distribution functions  $q_{i,0}^\gamma(x) \equiv q_i^\gamma(x, Q_0^2)$  at some scale  $Q_0^2$ .  $Q_0^2$  is usually chosen as the *smallest* value for which  $\alpha_s(Q_0^2)$  is sufficiently small to allow for a meaningful perturbative expansion.

Given these input distributions, the photonic parton densities, and thus  $F_2^\gamma$ , at different values of  $Q^2$  can be computed using the inhomogeneous evolution equations. In LO, they read [2, 11]:

$$\frac{dq_{\text{NS}}^\gamma(x, Q^2)}{d \log Q^2} = \frac{\alpha_{\text{em}}}{2\pi} k_{\text{NS}}^\gamma(x) + \frac{\alpha_s(Q^2)}{2\pi} (P_{qq}^0 \otimes q_{\text{NS}}^\gamma)(x, Q^2); \quad (8a)$$

$$\frac{d\Sigma^\gamma(x, Q^2)}{d \log Q^2} = \frac{\alpha_{\text{em}}}{2\pi} k_\Sigma^\gamma(x) + \frac{\alpha_s(Q^2)}{2\pi} [(P_{qq}^0 \otimes \Sigma^\gamma)(x, Q^2) + (P_{qG}^0 \otimes G^\gamma)(x, Q^2)]; \quad (8b)$$

$$\frac{dG^\gamma(x, Q^2)}{d \log Q^2} = \frac{\alpha_s(Q^2)}{2\pi} [(P_{Gq}^0 \otimes \Sigma^\gamma)(x, Q^2) + (P_{GG}^0 \otimes G^\gamma)(x, Q^2)], \quad (8c)$$

where we have used the notation

$$(P \otimes q)(x, Q^2) \equiv \int_x^1 \frac{dy}{y} P(y) q\left(\frac{x}{y}, Q^2\right). \quad (9)$$

The  $P_{ij}^0$  are the usual (LO)  $j \rightarrow i$  splitting functions and  $k_i^\gamma$  describe  $\gamma \rightarrow q\bar{q}$  splitting. Eq.(8a) describes the evolution of the nonsinglet distributions (differences of quark densities), i.e. re-sums only diagrams of the type shown in Fig. 2b, while eqs.(8b,8c) describe the evolution of the singlet sector ( $\Sigma^\gamma \equiv \sum_i q_i^\gamma + \bar{q}_i^\gamma$ ), which includes diagrams of the kind shown in Fig. 2c. Notice that this necessitates the introduction of a gluon density inside the photon  $G^\gamma(x, Q^2)$ , with its corresponding input distribution  $G_0^\gamma(x) \equiv G^\gamma(x, Q_0^2)$ .

It is crucial to note that, given non-singular input distributions, the solutions of eqs.(8) will also remain [10] well-behaved at all finite values of  $Q^2$ . This is true both in LO and in NLO [12]. On the other hand one clearly has abandoned the hope to make an absolute prediction of  $F_2^\gamma(x, Q^2)$  in terms of  $\Lambda_{\text{QCD}}$  alone. The solutions of eqs.(8) still show an approximately linear growth with  $\log Q^2$ ; in this sense eq.(5) remains approximately correct, but the functions  $a$  and  $b$  now do depend weakly on  $Q^2$  (approximately like  $\log \log Q^2$ ), and the  $x$ -dependence of  $b$  is *not* computable. This approximate linear growth of  $F_2^\gamma$  with  $Q^2$  has been experimentally confirmed quite nicely[13] as shown in Fig. 3 taken from Ref. [13]. Notice that *no* momentum sum rule applies for the parton densities in the photon as defined here. The reason is that these densities are all of first order in the fine structure constant  $\alpha_{\text{em}}$ . Even a relatively large change in these densities can therefore always be compensated by a small change of the  $\mathcal{O}(\alpha_{\text{em}}^0)$  term in the decomposition of the physical photon, which is simply the “bare” photon [with distribution function  $\delta(1-x)$ ].

Before discussing our present knowledge of and parametrizations for the parton densities in the photon, we briefly address a few issues related to the calculation of  $F_2^\gamma$ . As mentioned above, eqs.(7),(8) have been extended to NLO quite early, although a mistake in the two-loop  $\gamma \rightarrow G$  splitting function was found [14] only fairly recently. A full NLO treatment of massive quarks is now also available [15] for both  $F_2^\gamma$  and  $F_L^\gamma$ . A first treatment of small- $x$  effects

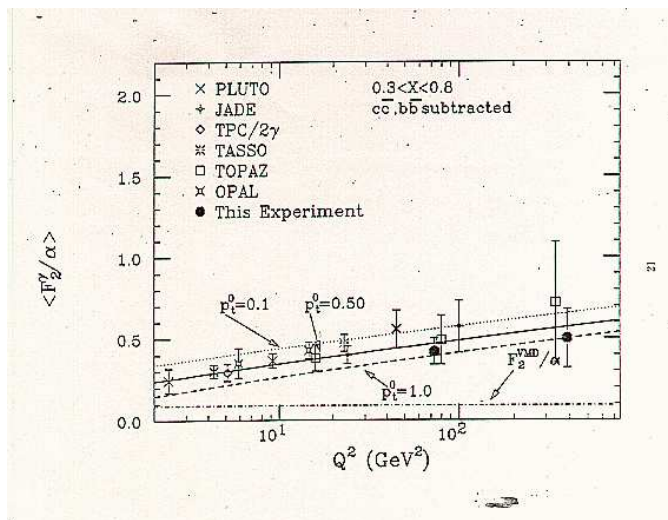


Figure 3:  $x$  averaged data on  $F_2^\gamma$  as a function of  $Q^2$ [13].

in the photon structure functions, i.e.  $\log 1/x$  re-summation and parton recombination, has been presented in ref.[16]; however, the predicted steep increase of  $F_2^\gamma$  at small  $x$  has not been observed experimentally [17]. Finally, non-perturbative contributions to  $F_2^\gamma$  are expected to be greatly suppressed if the target photon is also far off-shell. One can therefore derive unambiguous QCD predictions [18] in the region  $Q^2 \gg P^2 \gg \Lambda^2$ , where the first strong inequality has been imposed to allow for a meaningful definition of structure functions. However, it has recently been pointed out [19] that non-perturbative effects might survive longer than previously expected; an unambiguous prediction would then only be possible for very large  $P^2$ , and even larger  $Q^2$ , where the cross-section is very small.

### Parametrizations of Photonic Parton Densities:

As discussed above the  $Q^2$  evolution of the photonic parton densities  $\bar{q}^\gamma(x, Q^2) \equiv (q_i^\gamma, G^\gamma)(x, Q^2)$  is uniquely determined by perturbative QCD, eqs.(8) and their NLO extension once input distributions  $\bar{q}_0^\gamma$  at a fixed  $Q^2 = Q_0^2$  are specified. Though similar to the nucleonic case, the determination of the input distributions is much more difficult in case of the photon, for a variety of reasons.

To begin with, no momentum sum rule applies for  $\bar{q}_0^\gamma$ , as discussed above. This means that it will be difficult to derive reliable information on  $G_0^\gamma$  from measurements of  $F_2^\gamma$  alone: in LO, the gluon density only enters via the (subleading)  $Q^2$  evolution in  $F_2^\gamma$ . We will see below that parametrizations for  $G^\gamma$  still differ by sizable factors over the entire  $x$  range unless  $Q^2$  is very large.

Secondly, so far deep-inelastic  $e\gamma$  scattering could only be studied at  $e^+e^-$  colliders, where the target photon is itself radiated off one of the incoming leptons. The cross section from the measurement of which  $F_2^\gamma$  is to be determined is of order  $d\sigma/dQ^2 \sim \alpha_{\text{em}}^4 / (\pi Q^4) \log(E/m_e)$ , see eq.(2). The event rate is therefore quite small; the most recent measurements [6, 17, 20, 13] typically have around 1,000 events at  $Q^2 \simeq 5 \text{ GeV}^2$ , and the statistics rapidly gets worse at higher  $Q^2$ .

Another problem is that the  $e^\pm$  emitting the target photon is usually not detected, since it emerges at too small an angle. This means that the energy of the target photon, and hence the Bjorken variable  $x$ , can *only* be determined from the hadronic system. All existing analyses try to determine  $x$  from the invariant mass  $W$ , using eq.(4). Since at least some of the produced hadrons usually also escape undetected, the measured value of  $W$  ( $W_{\text{vis}}$ ) is generally *smaller* than the true  $W$ . One has to correct for this by “unfolding” the measured  $W_{\text{vis}}$  distribution to arrive at the true  $W$  ( and hence true  $x$  ) distributions. To do this one has to model the hadronic system  $X$ . Reasonably well tested algorithms have been evolved for this. The procedure normally used by the experimentalists is as originally suggested in Ref. [21]. However the way it is implemented currently [22, 17, 20, 13] has certain shortcomings [4, 23]. Also this procedure can lead to large uncertainties at the boundaries of the accessible range of  $x$  values. It has been shown explicitly [24] that different ansätze for  $X$  can lead to quite different “measurements” of  $F_2^\gamma$  at small  $x$ . The estimation of systematic error due to unfolding procedure only includes things like the choice of binning [17] and not some of the uncertainties in the modelling of the state  $X$ . This might help to explain the apparent discrepancy between different data sets [6]. Fortunately, new ideas for improved unfolding algorithms [25] are now under investigation; this should facilitate the measurement of  $F_2^\gamma$  at small  $x$ , especially at high energy (LEP2) [26] In spite of this, measurements of  $F_2^\gamma$  probably still provide the most reliable constraints on the input distributions  $\bar{q}_0^\gamma(x)$ ; they are certainly the only data that have been taken into account when constructing existing parametrizations of  $\bar{q}^\gamma(x, Q^2)$ .

At present there exist a large number ( $\sim 20$ ) parametrizations for the photonic parton densities. Apart from the simplest and the oldest parametrizations [27, 28] based on “Asymptotic” LO prediction [2, 29], (which were recently improved by Gordon and Storrow [30]) all other parametrizations involve some amount of data fitting. However, due to the rather large experimental errors of data on  $F_2^\gamma$ , additional *assumptions* always had to be made. The different parametrizations are not just different fits to the data but they differ from each other in these assumptions, the treatment of heavy quarks, choice of the scale  $Q_0^2$  and the physics ideas used for this choice of input densities. One assumption made by all of them is that quark and anti-quark distributions (of the same flavour) are identical, which guarantees that the photon carries no flavour.

The DG parametrization [31] was the first to start from input distributions and is based on only a single measurement of  $F_2^\gamma$  at  $Q^2 \simeq 5.2\text{GeV}^2$  that was then available. Two assumptions were made : All input quark densities were assumed to be proportional to the squared quark charges, i.e.  $u^\gamma = 4d^\gamma = 4s^\gamma$  at  $Q_0^2 = 1\text{ GeV}^2$ ; and the gluon input was generated purely radiatively. This parametrization only exists in LO. The charm content is definitely overestimated in this parametrization.

The LAC parametrizations [32] are based on a much larger data set. The main point of these fits was to demonstrate that data on  $F_2^\gamma$  constrain  $G^\gamma$  very poorly. In particular, they allow a very hard gluon, (LAC3), as well as very soft gluon distributions (LAC1, LAC2). The LAC parametrizations only exist for  $N_f = 4$  massless flavours and in LO. *No* assumptions about the relative sizes of the four input quark densities were made in the fit. LAC3 has been clearly excluded by data on jet production in  $ep$  scattering as well as in real  $\gamma\gamma$  scattering (see discussions at the end); the experimental status of LAC1,2 is less clear.

The recent WHIT parametrizations [33] follow a similar philosophy as LAC, at least

regarding the gluon input; however, their choices for  $G_0^\gamma$  are much less extreme. In the WHIT1,2,3 parametrizations, gluons carry about half as much of the photon’s momentum as quarks do (at the input scale  $Q_0^2 = 4 \text{ GeV}^2$ ), while in WHIT4,5,6 gluons and quarks carry about the same momentum fraction and in each set softness of the input gluon density was systematically increased. These only exist in LO, but great care has been taken to treat the ( $x$ -dependent) charm threshold correctly. This is much more important here than for nucleonic parton densities, since the photon very rapidly develops an “intrinsic charm” component from  $\gamma \rightarrow c\bar{c}$  splitting.

The GRV parametrization [34] is the first NLO fit of  $\bar{q}^\gamma$ ; a LO version is also available. This parametrization is based on the same “dynamical” philosophy where one starts from a very simple input at a very low  $Q_0^2$  (0.25 GeV<sup>2</sup> in LO, 0.3 GeV<sup>2</sup> in NLO); this scale is assumed to be the same for  $p$ ,  $\pi$  and  $\gamma$  targets. The observed, more complex structure is then generated dynamically by the evolution equations. The input densities for the photon are taken proportional to those for the (vector meson and hence) pion case[35]. Over and above the  $\gamma \rightarrow \rho$  transition probability given by the VDM there is a proportionality factor  $\kappa$  which is the *only* free parameter in this ansatz and was determined to  $\kappa = 2$  (1.6) in LO (NLO). This approach has met with some criticism due to the low scale used. The GRV parametrization ensures a smooth onset of the charm density, using an  $x$ -independent threshold.

The GS parametrizations [30] were developed shortly after GRV, but follow a quite different strategy. Problems with low input scales [36] are avoided by choosing  $Q_0^2 = 5.3 \text{ GeV}^2$ . This is certainly in the perturbative region, but necessitates a rather complicated ansatz for the input distributions:

$$\bar{q}_{0,\text{GS}}^\gamma(x) = \kappa \frac{4\pi\alpha_{\text{em}}}{f_\rho^2} \bar{q}_0^\pi(x, Q_0^2) + \bar{q}_{\text{QPM}}^\gamma(x, Q_0^2). \quad (10)$$

The free parameters in the fit are the momentum fractions carried by gluons and sea-quarks in the pion, the parameter  $\kappa$ , and the light quark masses. In the GS2 parametrization,  $G_0^\gamma$  is assumed to come entirely from the first term in eq.(10), while in GS1 the second term also contributes via radiation. While the fit gives reasonable values for all the three parameters, the ansatz (10) though true in the perturbative region is not invariant under the evolution equations. For practical purposes, however, it includes sufficiently many free parameters to allow a decent description of data on  $F_2^\gamma$ . The newer version uses of this parametrisation [37] uses slightly reduced input scale  $Q_0^2 = 3 \text{ GeV}^2$ , and for the first time includes data on jet production in two-photon collisions in the fit; unfortunately this still does not allow to pin down  $G^\gamma$  with any precision.

The AGF parametrization [38] is (in its “standard” form) quite similar to GRV. In particular, they also assume that at a low input scale  $Q_0^2 = 0.25 \text{ GeV}^2$  the photonic parton densities are described by the VDM. The main difference is in the scheme used for determining the input densities as well as inclusion of the  $\rho - \phi - \omega$  interference effects. Separate fits are provided for the “anomalous” (or “pointlike”) and “non-perturbative” contributions to  $\bar{q}^\gamma$ , allowing the user to specify the absolute normalization (although not the shape) of the latter.

Finally, two of the SaS parametrizations [23] are based on a similar philosophy as the GRV and AGF parametrizations, by assuming that at a low  $Q_0 \simeq 0.6 \text{ GeV}$  the perturba-



tive component vanishes (SaS1). However, while the normalization of the non-perturbative contribution is taken from the VDM the shapes of the quark and gluon distributions are fitted from data. Although the SaS parametrizations are available in LO only, the authors attempt to estimate the scheme dependence providing a parametrization (SaS1M) where the non leading-log part of the QPM prediction for  $F_2^\gamma$  has been added to eq.(7), while SaS1D is based on eq.(7) alone. There are also two parametrizations (SaS2D, SaS2M) with  $Q_0 = 2$  GeV; however, in this case the normalization of the fitted “soft” contribution had to be left free. The SaS1 sets preferred by the authors are quite similar to AGF; the real significance of ref.[23] is that it carefully describes the properties of the hadronic state  $X$  for both the hadronic and “anomalous” contributions, as needed for a full event characterization.

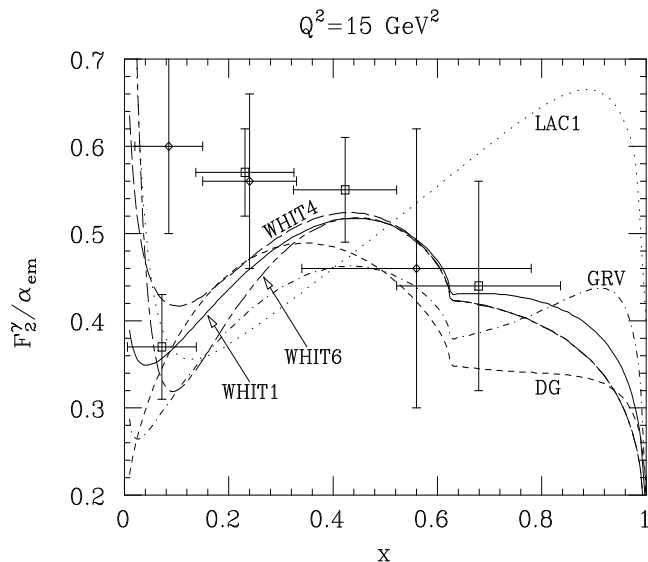


Figure 4: Data on  $F_2^\gamma$  [17, 20] as a function of  $x$  compared with various parametrizations

In Fig. 4 we compare various LO parametrizations of  $F_2^\gamma$  at  $Q^2 = 15$  GeV<sup>2</sup> with recent data taken by the OPAL [17] and TOPAZ [20] collaborations; present data are not able to distinguish between LO and NLO fits. In order to allow for a meaningful comparison, we have added a charm contribution to the OPAL data, as estimated from the QPM; this contribution had been subtracted in their analysis. We have used the DG and GRV parametrizations with  $N_f = 3$  flavours, since their parametrizations of  $c^\gamma$  are meant to be used only if  $\log Q^2/m_c^2 \gg 1$ ; the charm contribution has again been estimated from the QPM. <sup>§</sup> As discussed earlier, WHIT provides a parametrization of  $c^\gamma$  that includes the correct kinematical threshold, while LAC treat the charm as massless at all  $Q^2$ .

We see that most parametrizations give quite similar results for  $F_2^\gamma$  over most of the relevant  $x$ -range; the exception is LAC1, which exceeds the other parametrizations both at large and at very small  $x$ . It should be noted that the data points represent averages over the respective  $x$  bins; the lowest bin starts at  $x = 0.006$  (0.02) for the OPAL (TOPAZ) data. The first OPAL point is therefore in conflict [24] with the LAC1 prediction. Unfortunately there is also some discrepancy between the TOPAZ and OPAL data at low  $x$ . As discussed

<sup>§</sup>We have ignored the small contribution [15] from  $\gamma^*g \rightarrow c\bar{c}$  in this figure.

above, one is sensitive to the unfolding procedure here; for this reason, WHIT chose not to use these (and similar) points in their fit. (The other fits predate the data shown in Fig. 4.) This ambiguity in present low- $x$  data is to be regretted, since in principle these data have the potential to discriminate between different ansätze for  $G_0^\gamma$ . This can most clearly be seen by comparing the curves for WHIT4 (long dashed) and WHIT6 (long-short dashed), which have the *same* valence quark input, and even the same  $\int xG_0^\gamma dx$ : WHIT4 has a harder gluon input distribution, and therefore predicts a larger  $F_2^\gamma$  at  $x \simeq 0.1$ ; WHIT6 has many more soft gluons, and therefore a very rapid increase of  $F_2^\gamma$  for  $x \leq 0.05$ , not unlike LAC1. Finally, it should be mentioned that the GS, AGF and SaS parametrizations also reproduce these data quite well.

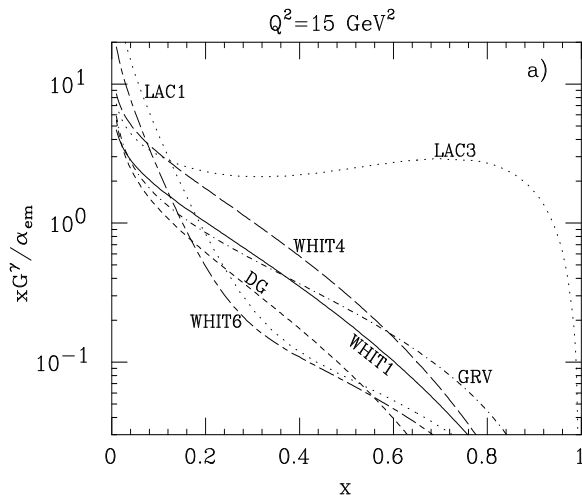


Figure 5: Gluon densities in various parametrisations of  $\vec{q}^\gamma$

Discriminating between these parametrizations would be much easier if one could measure the gluon density directly. This is demonstrated in Fig. 5, where we show results for  $xG^\gamma$  at the same value of  $Q^2$ ; we have chosen the same LO parametrizations as in Fig. 4, and included the LAC3 parametrization with its extremely hard gluon density. Note that, for example, WHIT4 and WHIT6 now differ by a factor of 5 for  $x$  around 0.3. The gluon distribution of WHIT6 is rather similar in shape to the one of LAC1, but significantly smaller in magnitude. Indeed, in all three LAC parametrizations, gluons carry significantly more momentum than quarks for  $Q^2 \leq 20$  GeV<sup>2</sup>; this is counter-intuitive [30], since in known hadrons, and hence presumably in a VMD-like low- $Q^2$  photon, gluons and quarks carry about equal momentum fractions, while at very high  $Q^2$  the inhomogeneous evolution equations (8) predict that quarks in the photon carry about three times more momentum than gluons. Notice finally that GRV predicts a relatively flat gluon distribution. This results partly from the low value of the input scale  $Q_0^2 = 0.25$  GeV<sup>2</sup>, compared to 1 GeV<sup>2</sup> for DG and 4 GeV<sup>2</sup> for WHIT and LAC1; a larger  $Q^2/Q_0^2$  allows for more radiation of relatively hard gluons off large- $x$  quarks.

Since the measurement of  $F_2^\gamma$  can not constrain the flavour structure, the different parametrizations mentioned above differ substantially from each other in their flavour struc-

ture as well.

Hard processes other than the DIS and  $\bar{q}\gamma$  :

The discussion at the end of the last section clearly shows that while the data on  $F_2^\gamma$  accumulated till now indeed supports the theoretical predictions, the DIS data cannot discriminate between the various parametrisations which differ considerably in their gluon content and flavour structure. In order to make use of the structure function language effectively to calculate processes involving photons, we need to improve upon this knowledge. Hard processes where the partons in the photon participate in the hard scattering, the so called ‘resolved processes’ [4] hold the promise of being able to do that and an experimental study of these processes has taken the centre stage in  $\gamma\gamma$  and  $\gamma p$  physics in the last 3-4 years. Both the  $\gamma\gamma$  scattering at TRISTAN and LEP as well as  $\gamma p$  scattering at HERA, has begun to provide a lot of data on jet production as well as heavy flavour production which have demonstrated ability to discriminate between different parametrisations of  $G^\gamma(x, Q^2)$ . See ref. [4] for a summary of the recent developments in the area. Here, I present only as an

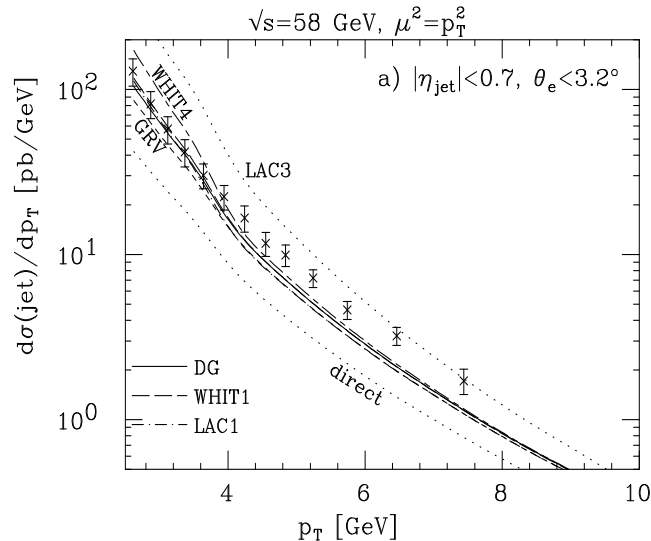


Figure 6: Single-jet inclusive cross-section in  $\gamma\gamma$  collisions obtained by TOPAZ [39] compared with predictions for various parametrisations of  $\bar{q}\gamma$

example of the available experimental information the inclusive single jet spectrum expected for the the anti-tagging conditions of the TOPAZ detector at TRISTAN (the TRISTAN data on jet production are the only published data where the detector effects have been unfolded) for various parametrisations mentioned above. The lower dotted curve shows the direct contribution only. Thus the data clearly demonstrate existence of the ‘resolved’ contributions. The other curves show LO predictions for the various parametrisations. It can be clearly seen that the data have some discriminatory power and rule out already the LAC3

parametrisation. The data from TRISTAN on heavy flavour (charm) production seem to disfavour DG parametrisation somewhat, whereas the jet production data from HERA also rule out LAC3. Further studies of jet and heavy flavour production at HERA, LEP as well as direct photon production at HERA can indeed provide some more information on the photonic parton densities.

## Conclusions:

- 1 The basic predictions of perturbative QCD as regards the  $Q^2$  and  $x$  dependence of  $F_2^\gamma$  have been confirmed by experiments. The only sensible way is to treat the  $F_2^\gamma$  similar to the nucleon structure function and fit the form of input densities at a low scale, using the data on  $F_2^\gamma$  and the evolution equations.
- 2 Various parametrisations of the photonic parton densities  $\bar{q}^\gamma$  exist all of which describe the data on  $F_2^\gamma$  well, but they differ a lot in the gluon densities  $G^\gamma(x, Q^2)$  as well as in their flavour structure. Data at small  $x$  from LEP2 might be able to distinguish between different parametrisations.
- 3 The ‘Resolved Photon Processes’, where the partons in the photon participate in the hard scattering also has the potential of providing important information about  $\bar{q}^\gamma$  in general and the gluon density in particular. Data from HERA ( $ep$  experiments) and TRISTAN/LEP ( $e^+e^-$  experiments) have already confirmed the existence of the ‘resolved photon’ processes at the expected level and have begun to provide nontrivial information on  $\bar{q}^\gamma$ .

## References

- [1] T.F. Walsh, Phys. Lett. **36B**, 121 (1971); S.M. Berman, J.D. Bjorken and J.B. Kogut, Phys. Rev. **D4**, 3388 (1971); P.M. Zerwas and T.F. Walsh, Phys. Lett. **44B**, 195 (1973).
- [2] E. Witten, Nucl. Phys. **B120**, 189 (1977).
- [3] PLUTO collab., Ch. Berger et al., Phys. Lett. **107B**, 168 (1981).
- [4] M. Drees and R.M. Godbole, Journal of Phys. G, Nucl. and Part. Phys., **21** 1559 (1995).
- [5] H. Abramowicz, K. Charchula, M. Krawczyk, A. Levy and U. Maor, Int. J. Mod. Phys. **A8**, 1005 (1993).
- [6] For a recent review of data on the production of hadronic final states in (real or virtual) two-photon collisions, see D. Morgan, M.R. Pennington and M.R. Whalley, J. Phys. **G20**, A1 (1994).
- [7] W.A. Bardeen and A.J. Buras, Phys. Rev. **D20**, 166 (1979); erratum, **D21**, 2041 (1980); D.W. Duke and J.F. Owens, Phys. Rev. **D22**, 2280 (1980).

- [8] G. Rossi, Phys. Lett. **130B**, 105 (1983); R.J. Buttery and J.K. Storrow, Mod. Phys. Lett. **A7**, 3229 (1992).
- [9] J.J. Sakurai and D. Schildknecht, Phys. Lett. **41B**, 489 (1972).
- [10] M. Glück and E. Reya, Phys. Rev. **D28**, 2749 (1983).
- [11] R.J. deWitt, L.M. Jones, J.D. Sullivan, D.E. Willen and H.W. Wyld, Phys. Rev. **D19**, 2046 (1979).
- [12] G. Rossi, Phys. Rev. **D29**, 852 (1984); M. Glück, K. Grassie and E. Reya, Phys. Rev. **D30**, 1447 (1984); M. Drees, Z. Phys. **C27**, 123 (1985).
- [13] AMY Collab., S.K. Sahu et al, Phys. Lett. **B 346**, 208 (1995).
- [14] M. Fontannaz and E. Pilon, Phys. Rev. **D45**, 382 (1992), and erratum: **D46**, 484 (1992); M. Glück, E. Reya and A. Vogt, Phys. Rev. **D45**, 3986 (1992).
- [15] E. Laenen, S. Riemersma, J. Smith and W.L. van Neerven, Phys. Rev. **D49**, 5753 (1994).
- [16] J.R. Forshaw and P.N. Harriman, Phys. Rev. **D46**, 3778 (1992).
- [17] OPAL collab., R. Akers et al., Z. Phys. **C61**, 199 (1994).
- [18] T. Uematsu and T.F. Walsh, Nucl. Phys. **B199**, 93 (1982).
- [19] M. Glück, E. Reya and M. Stratmann, Phys. Rev. **D51**, 3220 (1995).
- [20] TOPAZ collab., K. Muramatsu et al., Phys. Lett. **B332**, 477 (1994).
- [21] J.H. Field, F. Kapusta and L. Poggioli, Z. Phys. **C36**, 121 (1987); F. Kapusta, Z. Phys. **C42**, 225 (1989).
- [22] AMY collab., T. Sasaki et al., Phys. Lett. **B252**, 491 (1990).
- [23] G.A. Schuler and T. Sjöstrand, CERN-TH/95-62, hep-ph 9503384.
- [24] D.J. Miller, in the Proceedings of the *Workshop on Two-Photon Physics at LEP and HERA*, Lund, May 1994, eds. G. Jarlskog and L. Jönsson.
- [25] J.R. Forshaw and M.H. Seymour, Talk given at *Photon 95*, Sheffield, England, April 1995, CERN-TH/95-105, hep-ph 9505286; D.J. Miller, private communication.
- [26] Gamma Gamma Physics at LEP2 (hep-ph/9601317) P.Aurenche et al, To appear in the proceedings of the LEP2 workshop.
- [27] A. Nicolaidis, Nucl. Phys. **B163**, 156 (1980).
- [28] D.W. Duke and J.F. Owens, Phys. Rev. **D26**, 1600 (1982); erratum, **D28**, 1227 (1983).
- [29] C.H. Llewellyn Smith, Phys. Lett. **79B**, 83 (1978).

- [30] L.E. Gordon and J.K. Storrow, *Z. Phys.* **C56**, 307 (1992).
- [31] M. Drees and K. Grassie, *Z. Phys.* **C28**, 451 (1985).
- [32] H. Abramowicz, K. Charchula and A. Levy, *Phys. Lett.* **B269**, 458 (1991).
- [33] K. Hagiwara, M. Tanaka, I. Watanabe and T. Izubuchi, *Phys. Rev.* **D51**, 3197 (1995).
- [34] M. Glück, E. Reya and A. Vogt, *Phys. Rev.* **D46**, 1973 (1992).
- [35] M. Glück, E. Reya and A. Vogt, *Z. Phys. C* **D53**, 651 (1992).
- [36] L.E. Gordon, D.M. Holling and J.K. Storrow, *J. Phys.* **G20**, 549 (1994).
- [37] L.E. Gordon and J.K. Storrow, ANL report ANL-HEP-CP 95-37, to appear in the Proceedings of *Photon 95* [25].
- [38] P. Aurenche, J.-P. Guillet and M. Fontannaz, *Z. Phys.* **C64**, 621 (1994).
- [39] TOPAZ Collab. H. Hayashii et al, *Phys. Lett.* **B 314**, 149 (1993).